World Academy of Science, Engineering and Technology
International Journal of Energy and Power Engineering
Vol:9, No:6, 2015

A Theoretical Model for a Humidification Dehumidification (HD) Solar Desalination Unit

Yasser Elhenawy, M. Abd Elkader, Gamal H. Moustafa

Abstract**—**A theoretical study of a humidification dehumidification solar desalination unit has been carried out to increase understanding the effect of weather conditions on the unit productivity. A humidification-dehumidification (HD) solar desalination unit has been designed to provide fresh water for population in remote arid areas. It consists of solar water collector and air collector; to provide the hot water and air to the desalination chamber. The desalination chamber is divided into humidification and dehumidification towers. The circulation of air between the two towers is maintained by the forced convection. A mathematical model has been formulated, in which the thermodynamic relations were used to study the flow, heat and mass transfer inside the humidifier and dehumidifier. The present technique is performed in order to increase the unit performance. Heat and mass balance has been done and a set of governing equations has been solved using the finite difference technique. The unit productivity has been calculated along the working day during the summer and winter sessions and has compared with the available experimental results. The average accumulative productivity of the system in winter has been ranged between 2.5 to 4 (kg/m^2)/day, while the average summer productivity has been found between 8 to 12 (kg/m^2)/day.

Keywords**—**Finite difference, Dehumidification, Humidification, Solar desalination, Solar collector, Simulation, Water productivity.

I. Introduction

SOLAR desalination is a suitable solution to supply remote regions in Egypt and most other countries with fresh water. The standard techniques, like Multi-Stage Flash (MSF), Multi-Effect (ME), Vapor Compression (VC) and Reverse Osmosis (RO), are only reliable for large capacity ranges (100–50,000 m^3/day) of the fresh water production [1]. These technologies are expensive for small amounts of fresh water and also cannot be used in locations where maintenance facilities are limited. In addition, the use of conventional energy sources to drive these technologies has a negative impact on the environment. Solar desalination processes is a future promising technology. It has the following advantages: (i) solar energy is environmental friendly energy source; (ii) reduced operating costs and its simple structure so that it is suitable for a few families or small groups in remote areas, [2]. Solar desalination can either be direct or indirect. The direct solar humidification dehumidification desalination process (solar still) was investigated by [3]-[5].

The indirect solar HDD process has the advantage of separating the heating surface from the evaporation zone, and therefore the heating surface is relatively protected from corrosion or scale deposits. In fact, the humidification dehumidification desalination (HDD) is more costly than the conventional basin still solar desalination process [1]. Therefore, for the simplicity of design, a modest level of manufacturing technology is needed.

Very limited configurations of the HDD process have been developed. Yasser El Henawy et al. [6] investigated experimentally and theoretically the effect of main parameters on the productivity of the HDD process. Outdoor tests with input solar energy to the system were performed. The effect of weather conditions was considered, and the unsteady state performance of the system was found, therefore, examined. Ettouney [7] designed and analyzed various schemes of water desalination by humidification and dehumidification system. A theoretical investigation of a humidification - dehumidification desalination system configured by a double–pass flat plate solar air heater was examined by [8]. The effect of a cooling tower on the solar desalination system was studied by [9]. Dai et al. [10] reported the parametric analysis to improve the performance of a solar desalination unit with a humidification and dehumidification process. The performance analysis of the desalination unit of heat pump with humidification and dehumidification was studied by [11]. An experimental design and computer simulation of a multi-effect humidification dehumidification solar distillation was investigated by [12]. Fath and Ghazy [13] studied numerically a configuration that consists of a solar air heater, humidifier and dehumidifier. The feed water was not heated, and hence, the effect of water temperature was not considered. Darwish [14] suggested a system consisting of a solar pond, a humidifying column and a dehumidifying effect. They found that the effect of increasing air mass flow rate on the productivity is higher than that of the water mass flow rate. On the other hand, [15] reported that the feed water flow rate has a strong effect on the system productivity and the effect of the airflow rate is weak.

In the present article, a theoretical study of HDD unit has been considered. The unit consists of flat plate water and air solar collectors, storage tank and a dehumidifier. The aim is to develop a simulation program that able to analyze the characteristics of the humidification-dehumidification desalination unit to study the effect of operating and design

Yasser ElHenawy is with the Department of Mechanical Power Engineering, Faculty of Engineering, Port Said University, Egypt. (Corresponding author to provide phone: 002-01207302363; fax: (+02) (066) 3400936; e-mail: zicus2010@ yahoo.com).

M. Abd ElKader is with the Department of Mechanical Power Engineering, Faculty of Engineering, Port Said University, Egypt. (E-mail: mbeshary@yahoo.com).

Gamal H. Moustafa is with the Department of Mechanical Power Engineering, Faculty of Engineering, Port Said University, Egypt.

parameters as well as weather conditions on the unit performance and fresh water productivity.

II. System Description

A solar desalination unit with a humidification and dehumidification cycle is given in Fig. 1. It is configured mainly by a flat plate solar water collector, a v-shaped solar air collector, a humidifier and a dehumidifier. Seawater is heated by the solar water collector and sprayed by a sprinkler to form a falling film at the surface of the honeycomb wall in the humidifier (Fig. 2). It consists of a porous and durable honeycomb backing; characterized by a large evaporation surface per unit volume of the packed material. The air is heated by the solar air collector and forced through the humidifier where it becomes hot and humid due to the heat and mass exchanging between the seawater and air. Then, the humid air is cooled by the cold seawater as passing through the dehumidifier at which the water vapor condenses and turns into fresh water. The dehumidifier is a helix-tube type one. The cold seawater flows inside the tube and the fresh water is produced from the condensate on the dehumidifier surface. The remaining seawater drawn from the humidifier is cooled and collected at the bottom basin. Some of the water is fed to the solar collector again since it is not very concentrated and is still warm. Thus, the fresh water can be continually produced.

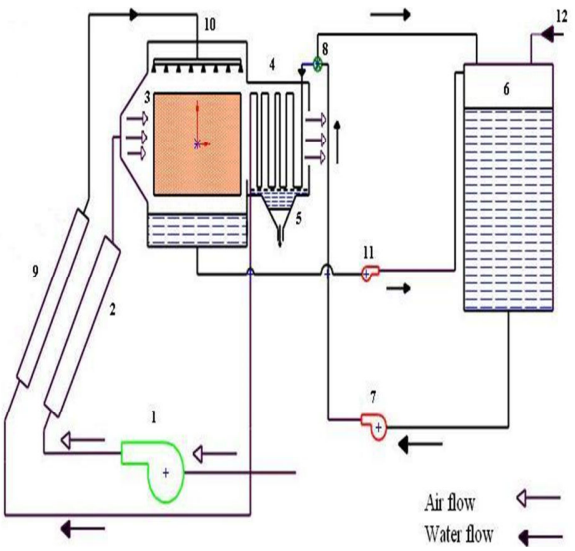

Fig. 1 A Schematic diagram of desalination system. 1. Blower, 2. Solar air collector, 3. Humidifier, 4. Dehumidifier, 5. Distilled water, 6. Seawater tank, 7. Feed pump, 8. Valve, 9. Solar water collector, 10. Sprinkler, 11. Drain pump, 12. Makeup of seawater.

III. Mathematical Model

A mathematical model of the unit is presented, in which the thermodynamic relations have been used to describe the flow, heat and mass transfer inside the humidifier, dehumidifier, and water and air solar collectors. A set of partial differential governing equations has been considered and solved using a finite difference technique. A computer program is developed and the following assumptions are considered: (i) the feed water, cooling water and feed air have constant flow rates along the day. (ii) Thermal losses due to the ambient are neglected. (iii) The thermal analysis is assumed in quesi-steady condition.

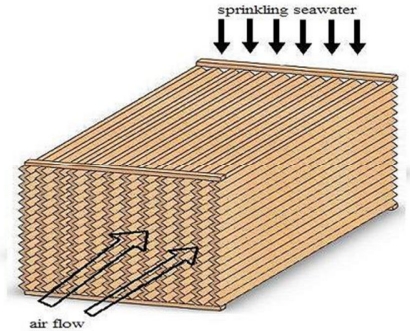

Fig. 2 A Sketch of honey-comb packing material in the humidifier

A. The Flat Plate Solar Water Collector

The thermal energy balance of the solar collector is written as [16]:

$$G_t \times A_{cl} = Q_{loss} + Q_u \tag{1}$$

where G_t is the total solar intensity (W/ m^2), Acl is the collector surface area (m^2), Q_{loss} is the heat loss from the collector and Q_u is the useful heat transferred from the absorber to water. Q_{stg} is the energy stored in the collector. The heat loss is expressed by [17]:

$$Q_{loss} = A_{cl} U_L \left(T_p - T_a\right) \tag{2}$$

where T_p and Ta are the average flat plate and ambient temperatures (K). The overall heat transfer coefficient of the collector UL (W/m^2) is the summation of three values of heat transfer coefficients, at the top U_t, bottom U_b, and side walls U_{si} [17].

$$U_L = U_t + U_b + U_{si} \tag{3}$$

where

$$U_b = \frac{1}{\left(\frac{\delta_{i,b}}{K_i} + \frac{\delta_{b,b}}{K_b}\right)} \cdot \frac{A_b}{A_{cl}} \quad U_{si} = \frac{1}{\left(\frac{\delta_{i,s}}{K_i} + \frac{\delta_{b,s}}{K_b}\right)} \cdot \frac{A_s}{A_{cl}} \tag{4}$$

where A_s and A_b are the side and bottom collector areas (m^2). The top heat transfer coefficient U_t is calculated from an empirical equation suggested by [17]:

$$U_t = \left[1 - (\zeta - 45)(0.00259 - 0.00144\,\varepsilon_p)\right] \left\{ \frac{1}{N/\left[(344/T_p)\left\{(T_p - T_a)/(N+f)\right\}^{0.31}\right] + 1/h_{win}} + \frac{\sigma\left(T_p^4 - T_a^4\right)/\left(T_p - T_a\right)}{\left[\varepsilon_p + 0.0425N\left(1-\varepsilon_p\right)\right]^{-1} + \left[(2N+f-1)/\varepsilon_g\right] - N} \right\} \tag{5}$$

where ζ is the collector tilt angle, N is the number of glass plate, ε_g and ε_p are the emittance of glass and absorber plate, T_p and Ta are the average plate and ambient temperatures. The term σ is the Boltzmann constant. The term f is given as:

$$f = \left(1 - 0.04h_{win} + 5\times10^{-4} h_{win}^{\ 2}\right)\left(1 + 0.058N\right) \quad (6)$$

where h_{win} is the wind heat transfer coefficient which is given by, $h_{win} = 5.7 + 3.5C_{win}$ where, C_{win} is the wind speed (m/s). The collector efficiency factor F_{cl} is estimated by,

$$F_{cl} = \frac{1}{SU_L\left[\frac{1}{U_L\left[D_o + (S - D_o)\eta_f\right]} + \frac{1}{C_{bond}} + \frac{1}{\pi D_i h_{tf}}\right]} \quad (7)$$

where S is the tube spacing (m), Di and Do are the inner and outer diameters of the collector tubes (m). The collector fin efficiency η_f is calculated by [17]:

$$\eta_f = \frac{\tanh\left[\sqrt{U_L / K_p \delta_p}\left(S - D_o\right)/2\right]}{\left[\sqrt{U_L / K_p \delta_p}\left(S - D_o\right)/2\right]} \quad (8)$$

For the flow with (Re<2300), the convective heat transfer coefficient h_{tf} and Prandtl number, Pr are given by [16]:

$$h_{tf} = 1.86\frac{K_f}{D_i}(\mathrm{Re\ Pr})^{1/3}\left(\frac{D_i}{L}\right)^{1/3}\left(\frac{\mu_f}{\mu_{f,t}}\right)^{0.14} \quad (9)$$

The Reynolds number (Re) and Prandtl number (Pr) are given by [17]:

$$\mathrm{Re} = \frac{4\dot{m}A_{cl}}{\pi D_i N_t \mu_f} \quad \mathrm{Pr} = \frac{\mu_f C_{p,f}}{K_f} \quad (10)$$

where k_f (W/mk), μ_f (N.s/m^2) and C_p (J/kg k) the thermal conductivity, dynamic viscosity and specific heat of the fluid are respectively. L is the tube length (m). The absorbed solar radiation (q_{abs}) is determined by, [18]:

$$q_{abs} = G_t(\tau\alpha)_{avg} \quad (11)$$

where τα is the average transmittance of the cover plate and absorptance of the absorbed plate. Also the heat removal factor (FR) is calculated from, [17]:

$$F_R = \frac{\dot{m}C_p}{U_L}\left[1 - e^{-U_L F_{cl}/\dot{m}C_p}\right] \quad (12)$$

where $\dot{m}$ is the mass flow rate per unit area of the collector (kg/sm^2). The useful energy from the collector is calculated from [17]:

$$Q_u = A_{cl}F_R\left[q_{abs} - U_L\left(T_{f,i} - T_a\right)\right] \quad (13)$$

and the average fluid temperature is thus obtained as [17]:

$$T_{f,a} = T_{f,i} + \frac{Q_u}{A_{cl}F_R U_L}\left[1 - \frac{F_R}{F_{cl}}\right] \quad (14)$$

The average plate temperature is obtained from [17]:

$$T_p = T_{f,o} + \frac{Q_u / N_t}{\left[\frac{1}{\pi h_{tf} D_i L} + \frac{1}{C_{bond} L}\right]^{-1}} \quad (15)$$

where N_t is the number of tubes and C bond is the conductive resistance of the bond. The fluid temperature at the outlet from the collector is calculated from [17]:

$$T_{f,o} = T_{f,i} + \frac{Q_u}{\dot{m}C_p} \quad (16)$$

The collector efficiency is determined by, [18]:

$$\eta_c = \frac{Q_u}{A_{cl}G_t} \quad (17)$$

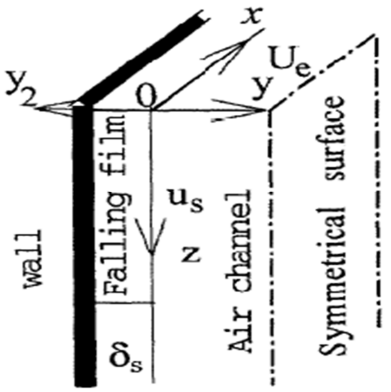

Fig. 3 Coordination set-up

B. Humidifier Modeling

The humidifier consists mainly of honeycomb packing material which is characterized by a large evaporation surface per unit volume. The mathematical model of the humidifier, which is established on the basis of energy and mass balances, is presented. The heat and mass transfer between the liquid film and the moist air is considered. The set of governing two dimensional equations is solved using the finite-difference method. The following assumptions are: (i) the flow of falling film is laminar and no wavy movement takes place at the water-air interface. (ii) the flow rate of falling film is believed constant because the evaporation rate of water out of the water-air interface is small enough. Fig. 3 shows the coordination set-up pleased along the interface line.

1. Governing Equations of Falling Film

If the liquid film falls slowly and steadily just under the gravity force, particularly in laminar flow, the mean velocity of the falling film, u_s is given as [10]:

$$u_s = \frac{\rho_s g \delta_s^2}{3\mu_s} \tag{18}$$

The thickness δ_s, is given as [10]:

$$\delta_s = \left[\frac{3\Gamma\mu_s}{g\rho_s^2}\right]^{1/3} \tag{19}$$

where Γ is the mass flow rate of saline water per unit width of the wall (kg/s.m) and g is the acceleration of gravity, m/s^2. The energy balance for the falling film is

$$u_s \frac{\partial T_s}{\partial z} = \alpha_s \frac{\partial^2 T_s}{\partial y_2^2} \tag{20}$$

2. Governing Equations of Moist Air:

The governing equations, including mass, momentum, and energy conservations are listed as follows [10]:

$$\frac{\partial u}{\partial x} + \frac{\partial v}{\partial y} = 0 \tag{21}$$

$$u\frac{\partial u}{\partial x} + v\frac{\partial u}{\partial y} = \gamma_a \frac{\partial^2 u}{\partial y^2} - \frac{1}{\rho_a}\frac{\partial p}{\partial x} \tag{22}$$

$$u\frac{\partial T}{\partial x} + v\frac{\partial T}{\partial y} = \alpha_a \frac{\partial^2 T}{\partial y^2} \tag{23}$$

The boundary conditions at the water - air interface:

$$y = \frac{d}{2} - \delta_s, u = u_e, \frac{\partial u}{\partial y} = 0, T = T_e$$

where ue (m/s) and Te (K) are the velocity and temperature of the incoming air.

$$u = 0, T = T_n, and\ T_s = T_n,$$
$$\alpha_a \frac{\partial T}{\partial y}\Big|_{y=0} = -\alpha_s \frac{\partial T_s}{\partial y_2}\Big|_{y_2=0} + \frac{\lambda W_j}{\rho_s C_{ps}}$$

where Tn and Ts are the interface and saline water temperatures, Wj and λ are the evaporation rate and latent heat of water. Solving the set flow equations (21)-(23) with boundary conditions, the distribution of the flow velocity and temperature inside the humidifier has been obtained. To simplify the above solution, auxiliary equations are needed.

Auxiliary Equations: The evaporation rate at the water surface is estimated from, [19]:

$$Wj = \varepsilon_1 (P_s - P_v)\left\{\frac{M}{2\pi RT_n}\right\}^{1/2} \tag{24}$$

Here M is the molecular weight of water and R is the universal gas constant, ε1 is the Knudsen coefficient of evaporation. It is calculated from: ε1 = (2ε)/(2-ε). The coefficient of evaporation, ε is calculated from:

$$\varepsilon = h^* \left[\frac{2\pi RT_s}{M}\right]^{1/2}\left[\frac{T_n}{\rho_v \lambda^2}\right] \tag{25}$$

The coefficient of heat transfer h (W/m^2 K) is given by, [18]:

$$h = \xi V^{\beta} \quad \text{W/m}^2\,^{o}\text{C} \tag{26}$$

The terms ξ and β are function of the plate spacing. For a 6.7mm plate spacing the values of ξ and β are 54 and 0.7 respectively. As the plate spacing increases to 13.4 mm, the values of ξ and β are changed to be 49 and 0.6.

Taking the phenomenon of evaporation into account, introduced the concept of the wet bulb coefficient of heat transfer (h*,W/m^2 K) to correct the heat transfer process of a wet surface:

$$h^* = h\left(1 + e\lambda / C_{pa}\right) \tag{27}$$

where h (W/m^2 ^{o}C) is the heat transfer coefficient and e is constant, given by:

$$e = \left(\omega_{\max} - \omega_{\min}\right)/\left(T_{\max} - T_{\min}\right) \tag{28}$$

Here T_{max} and T_{min} are the maximum and minimum temperatures at the water-air interface. T_{max} is the higher one of the temperatures of airflow and water flow. T_{min}, is the wet bulb temperature of the air. ω_{max} and ω_{min} are the maximum and minimum humidity corresponding to T_{max} and T_{min}.

C. Dehumidifier Modeling

The energy balance between the cooling water and air/condensing vapor stream is made. The energy balance is based on two following thermal equations [7]:

$$\dot{m}_{cw} C_{pcw}\left(T_{cwo} - T_{cwi}\right) = \dot{m}_a \left(H_o - H_i\right) \tag{29}$$

$$\dot{m}_{cw} C_{pcw}\left(T_{cwo} - T_{cwi}\right) = U_c A_c LMTD_c \tag{30}$$

where m_{cw}, and ma (kg/s are the mass flow rates of cooling water and incoming air. T_{cwo} and T_{cwi} (K) are the temperatures of cooling water at inlet and outlet. Hi and Ho (Kj/kg) are the enthalpy of air at inlet and outlet. In (30) the logarithmic mean temperature difference and the overall heat transfer coefficient are given by [7]:

$$LMTD_c = \frac{(T_{ac} - T_{cwo}) - (T_{ac} - T_{cwi})}{\ln\left(\frac{(T_{ac} - T_{cwo})}{(T_{ac} - T_{cwi})}\right)} \quad (31)$$

$$\frac{1}{U_c} = \frac{1}{h_{ci}}\frac{r_{co}}{r_{ci}} + Rf_c + \frac{r_{co}\ln\left(\frac{r_{co}}{r_{ci}}\right)}{k_c} + \frac{1}{h_{co}} \quad (32)$$

The production of distilled water (md) is given by

$$m_d = \dot{m}_a(\omega_o - \omega_i) \quad (33)$$

where ω_o and ω_i are the absolute humidity (kg H_2O/kg dry air) of air at the inlet and outlet from the dehumidifier.

D. V-groove Solar Air Collector

The v-shaped flat plate solar air collector is designed, Fig. 4. The calculations for the solar air collector are made with the following assumptions: (i) performance is steady state; (ii) There is no absorption of solar energy by a cover in so far, (iii) The radiation coefficient between the two air duct surfaces is found by assuming a mean radiant temperature equal to the mean fluid temperature. (iv) Loss through front and back sides are at the same temperature. The energy balances for the glass cover, absorber plate, and Fluid medium of the collector are given as follows: [20]

Glass cover:

$$U_t (T_g - T_a) = h_1 (T_p - T_g) + h_r (T_p - T_g) \quad (34)$$

V-groove absorber:

$$\tau_g \alpha_p G_t = h_1(T_p - T_g) + h_r (T_p - T_g) + h_2(T_p - T_f) \quad (35)$$

Fluid medium:

$$h_2 (T_p - T_f) + U_b (T_a - T_f) = \left(\frac{\dot{m} C_{air}}{W}\right)\left(\frac{dT_{air}}{dx}\right) \quad (36)$$

Solving (5), (6) with (34), (35) and (36), the air, absorber plate temperature and heat transfer coefficient have been obtained. The pressure drop through the channel in the air heater has been computed using the [20]:

$$\Delta P = \left[f_o + y\frac{D}{L}\right]\left(\frac{\dot{m}_{air}^2}{\rho}\right)\left(\frac{L}{D}\right)^3 \quad (37)$$

For the laminar flow (Re < 2550), f_o =24/Re, y = 0.9

For transitional flow (2550 < Re < 10^4)

$$f_o = 0.0094,\ y=2.92\ Re^{0.15}$$

For turbulent flow (10^4 <Re<10^5)

$$f_o = 0.059\ Re^{0.2},\ y = 0.73$$

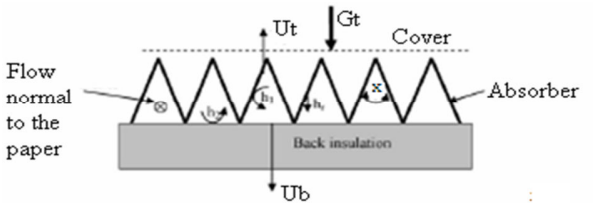

Fig. 4 A corrugated solar air collector

IV. The Solution Procedure

The procedure is as follows:

1. The input data, such as the mass flow rates of air, feed seawater, cooling water are known. In addition, the inlet air temperature and humidity are given.
2. The air and water temperature were obtained.
3. The fresh water from the humidifier was collected.

V. Results and Discussion

The characteristics of the humidification dehumidification solar desalination unit are theoretically performed and sample of data are presented. A comparison with available data is given.

The solar intensity along an operated summer day from 9 O'clock morning to 18 O'clock afternoon is given in Fig. 5. The water productivity in the same interval is also shown. The peak of solar intensity is shown at the middle of the day, around 13 O'clock. It decreases forward afternoon. At the beginning, 9 O'clock, there is no water productivity. As the solar intensity increases up to 13 O'clock the water productivity is increased. Afternoon, it decreases as the solar intensity is decreased.

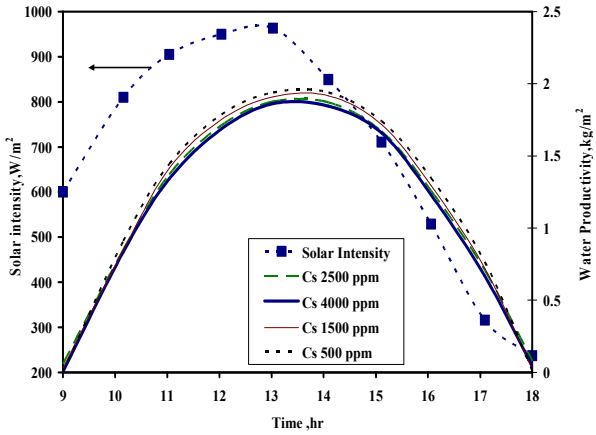

Fig. 5 Variation of solar intensity with different concentration on water productivity along an operating day

Fig. 6 shows the accumulative productivity along the operating day. The productivity increases and the accumulative productivity along the day of 22/7/2009, is about 12 kg/m2/day. In the real outdoor operation system, a delay time is to be between the starting of the running time and the

starting of fresh water production. It is also noticed that most of the energy received in the early hours is used as a sensible heat to warm up the test rig metal and the fluid flow.

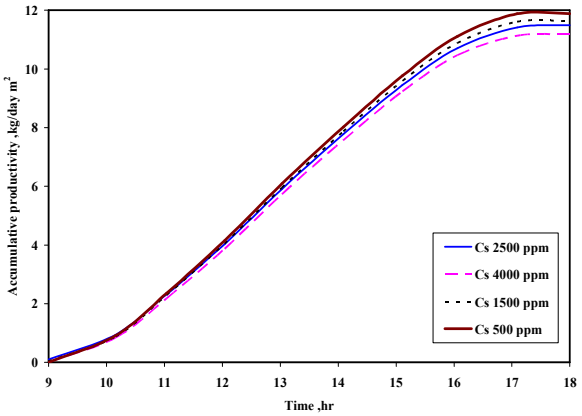

Fig. 6 Variation of accumulative productivity as a function of C_s

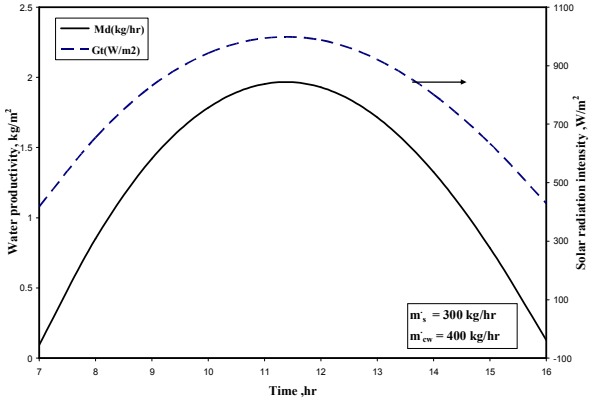

Fig. 7 Variation of solar intensity on water productivity along an operating day

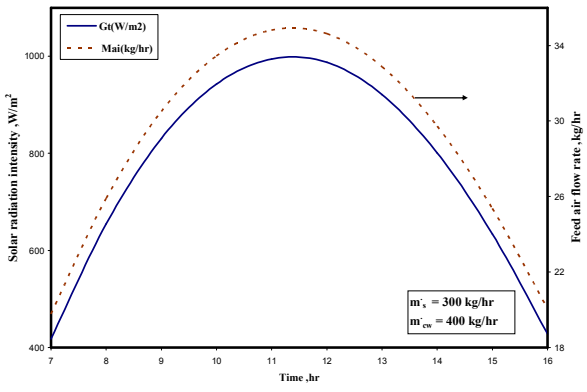

Fig. 8 Variation of solar intensity and feed airflow rate along an operating day

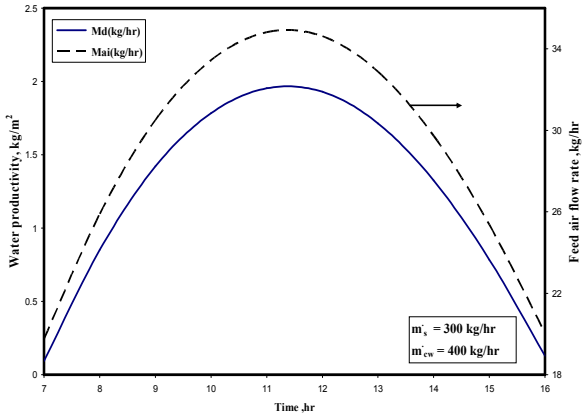

Fig. 9 Variation of feed airflow rate on water productivity along an operating day

The variation of estimated water productivity and solar radiation intensity along the operated day are given in Fig. 7. It is noted that the numerical model has reproduced successfully the characteristics of the HDD unit and the present results are agree well with published data.

The variation of estimated feed airflow rate from the solar air collector along an operating day is depicted in Fig. 8. It is noted that the numerical model has successes to reproduce the characteristics of the solar air collector.

Fig. 9 shows the variation of water productivity and feed airflow rate along the operated day. The fresh water productivity increases as the operating time increases from the 9 O'clock morning towards the middle of the operating day. The maximum flow rate is shown around 13 O'clock noon. It decreases as the solar intensity decreases afternoon.

The ambient conditions have also an influence on the system performance since the unit runs in an open-cycle mode. Fig. 10 shows the effect of the inlet temperature and relative humidity of air on the calculated feed airflow rate and water productivity. The results agree with the common knowledge in literature that the higher inlet temperature and humidity are beneficial for producing more fresh water. The water productivity of the unit increases as the inlet temperature is increased. In addition, the relative humidity of the air has a strong effect on the productivity of the unit. The water productivity increases with the increase of the relative humidity of the air.

Fig. 11 shows the effect of the humidifier inlet water temperature on the unit productivity. The water productivity decreases with increasing the water flow rate. This can be explained as follows: increasing the water flow rate leads to a decrease of the enthalpy of air. Hence, the ability to extract vapor from the air is decreased. As the feed water temperature is increased, the water productivity is increased for all values of the feed water flow rates.

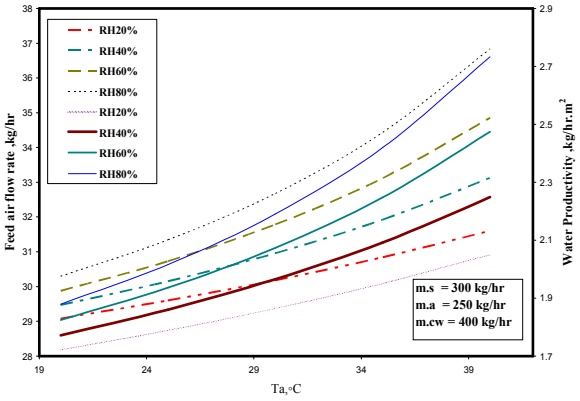

Fig. 10 Variation of temperature and feed airflow rate on water productivity along an operating day

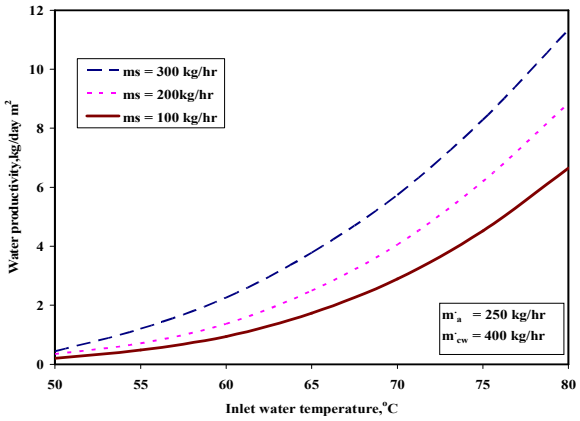

Fig. 11 Variation of temperature and feed water flow rate on water productivity along an operating day

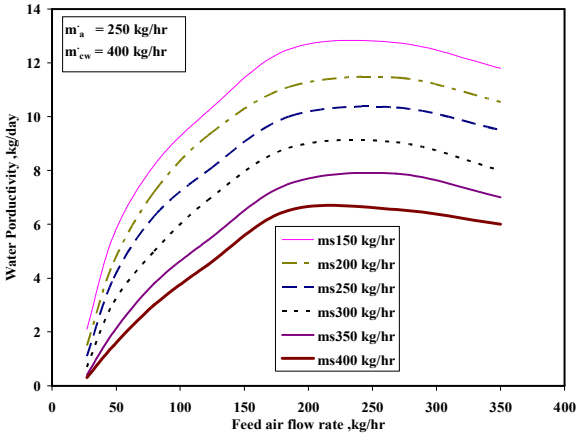

Fig. 12 Variation of feed airflow rate and on water productivity along an operating day

The variation of water productivity with the inlet air mass flow rate is given in Fig. 12 at different values of the feed water flow rates. It is seen that the water productivity gradually increases with the feed air flow rate up to a certain values and then slightly decreases or remains constant. The same results are shown with increasing the feed water mass flow rate (Fig. 13).

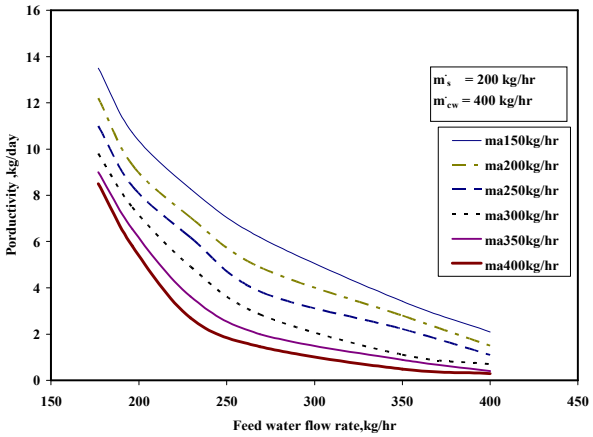

Fig. 13 Variation of feed water flow rate on water productivity along an operating day

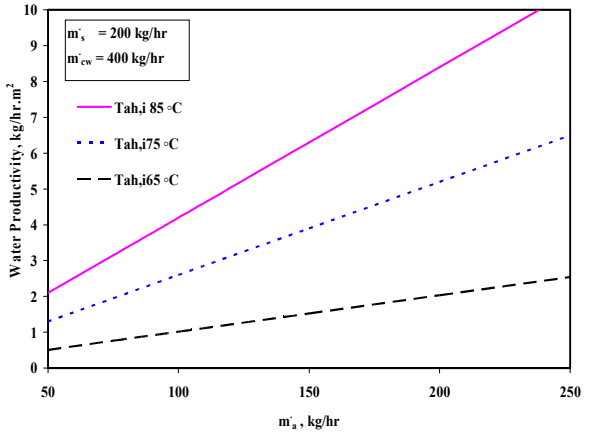

Fig. 14 Variation of feed water flow rate and temperature on water productivity along an operating day

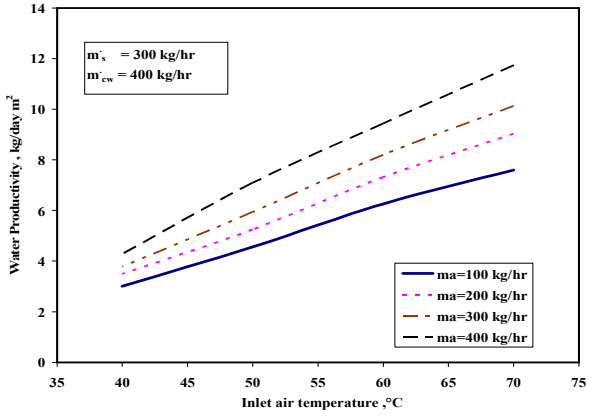

Fig. 15 Variation of inlet air temperature on water productivity along an operating day

The variations of water productivity with the inlet air mass flow rate and air temperature are given in Figs. 14 and 15. The variation is approximately linear. The ability of air to carry the

water vapor increases with the increase of the inlet air temperature.

The variation of water prodicitivity with the cooling water temperature along three days in summer 2009 is given in Fig. 16. The water productivity increases starting from 9 O'clock mooring up to 13 O'clock noon. Then it decreases forward. As the cooling water increase the water productivity is decreased.

Fig. 17 shows the effect of the solar water and air collector areas on the unit water productivity. The water productivity increases almost linearly with an increase in both the solar water and air collector areas.

The effect of tilt angle variations on the solar desalination unit was theoretically investigated. Figs. 18 and 19 illustrate that the productivity increases as the tilt angle increases during winter season however in summer as the cover slope decreases the productivity is increased. These results are attributed to the lower declination angle of the incident solar energy in winter season and the higher declination angle in summer.

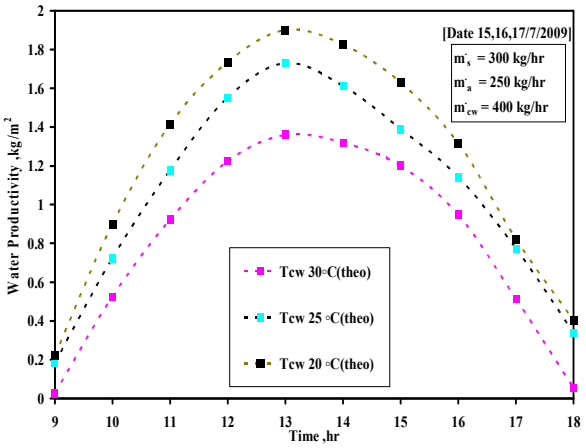

Fig. 16 Variation of cooling water temperatures on water productivity through three days

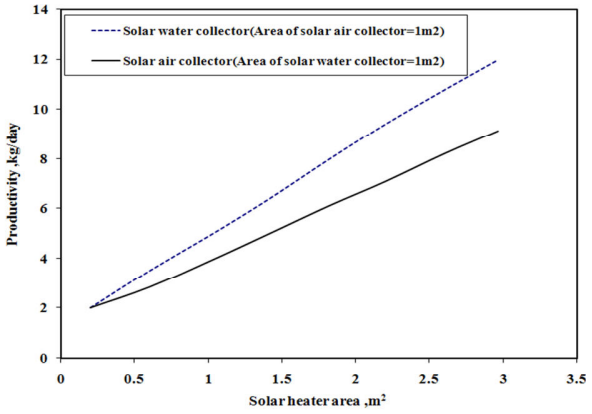

Fig. 17 Effect of the solar water and air collector areas on the unit water productivity

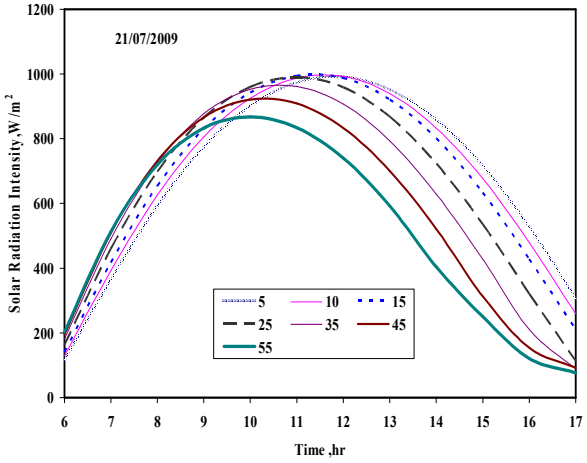

Fig. 18 Effect of the collector tilt angle on the solar radiation unit in winter

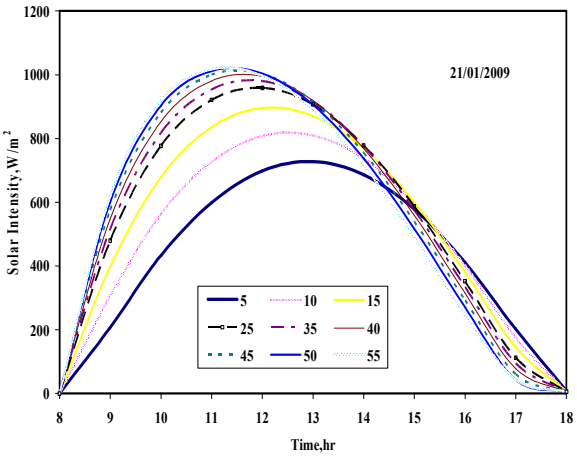

Fig. 19 Effect of the collector tilt angle on the solar radiation unit in summer

The variation of water productivity as a function of the packing materials is given in Fig. 20. The total surface area of the packing is kept constant. The water productivity is higher as used the wooden material. This indicates that the wetted area differs with changing the packing material and the wooden material is shown to give higher water productivity.

A comparison between the numerical and measured water productivity is given in Fig. 21. A good agreement is depicted. The trend of the variation of water productivity along the operating day is the same. The numerical model represents successfully the variation of water productivity for all different test conditions.

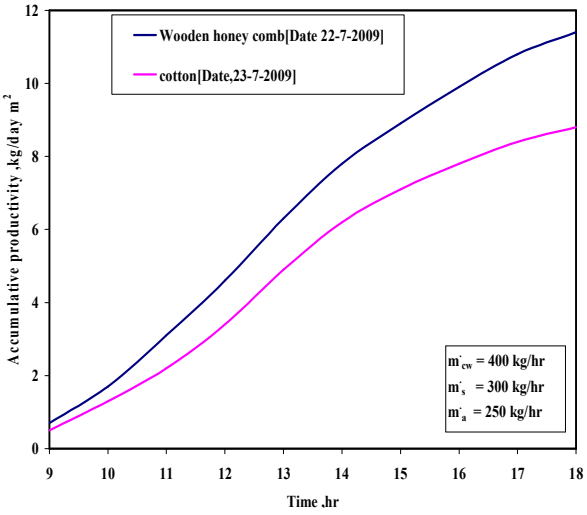

Fig. 20 Hourly accumulative productivity 22,23/7/2009

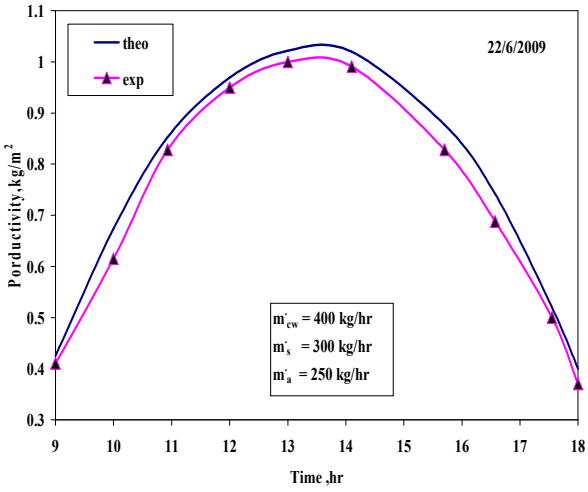

Fig. 21 Hourly productivity of the test rig during 22/7/2009

VI. Conclusions

A humidification - dehumidification (HDD) solar desalination unit has been simulated using a numerical finite difference model in order to optimize the unit performance. The system consists of an insulated desalination chamber coupled with a solar collector. The desalination chamber divided into humidifier tower and dehumidifier tower. The system was found to be suitable to provide drinking fresh water for population and remote arid areas. The main conclusions are:

1. A mathematical model was designed to predict the system productivity under different and wide range of operating conditions.
2. It is found that the accumulative productivity increases with the increase of inlet air temperature and relative humidity.
3. Increasing the seawater flow rate leads to decrease in water productivity to a certain value depending on the collector efficiency.
4. The optimum tilt angle which gives maximum solar radiation is found between 35:45^o in winter and 15:20^o in the summer.
5. The fresh water productivity of the unit is increasing with the wooden material and decreased with cotton material.
6. The results of the proposed mathematical model are in good agreement with those of the experimental model of the system.
7. The system daily productivity in summer is about 8 to 12 kg/m^2 day, and about 2.5 to 4 kg/m^2 day in winter.

Nomenclature

Symbols

d	Mean wall spacing, m
K	Thermal conductivity (W/m K)
Ps	Saturated water vapor pressure, Pa
Pv	Water vapor pressure of the air, Pa
Vh	Volume of packing materials in the humidifier, m^3
u,v	Velocity, m/s
h	Heat transfer coefficient, W/(m^2.s)
r	Radius ,m
RH	Relative humidity
Rf	Fouling resistance, m^2 ^{o}C/kW

Greek

δ	Thickness (m)
α	Thermal diffusivity , m^2/s
γ	Kinematic viscosity, m^2/s
λ	Latent heat of water, kJ/kg
μ	Dynamic viscosity, N/m^2.s
ρ	Density, kg/m^3
ε	Coefficient of evaporation
υ	V-groove angle of solar air heater , degree

Subscripts

b	Bottom, box
c	Dehumidifier
cw	cooling water
i	Inlet state, insulation
s	Saline water
si	Side
p	Plate
n	Liquids interface
o	Outlet
v	Water vapor

References

[1] Fath H.E., "Desalination Technology- The Role of Egypt in Region", IWT C, Alexandria, Egypt, 2000.
[2] Fath H.E., "Solar Desalination Promising Alternative for Fresh Water Production with Free Energy Simple Technology and Clean Environmental", Desalination, Vol. 116, pp. 45–56, 1998.
[3] M. Abdelkader, Nafey A. S., Abdelmotalip A., and Mabrouk A. A., "Parameters Affecting Solar Still Productivity", Energy Conversion and Management, Vol.411,pp 797–809, 2000.
[4] M.Abdelkader., Nafey A. S, Abdelmotalip A., and Mabrouk A.A., "Solar Still Productivity Enhancement", Energy Conversion and Management, Vol. 42, pp. 1401–1408,2001.
[5] M. Abdelkader., Nafey A. S, Abdelmotalip A., and Mabrouk A. A., "Enhancement of Solar Still Productivity Using Floating Perforated Black Plate", Energy Conversion and Management, Vol. 43 (7),pp.937-946,2002.
[6] Yasser ElHenawy, M. Abd ElKader, Aref., A., Gamal H. Moustafa "A Theoretical and Experimental Study for a Humidification –

Dehumidification (HD) Solar Desalination Unit" International Journal of Water Resources and Arid Environments, Vol.3(2),pp.108-120, ISSN 2079-7079,2014.

[7] Ettouney, H, "Design and Analysis of Humidification Dehumidification Desalination Process", Desalination, Vol. 183, pp.341–352, 2005.

[8] Yamali, C., and Solmus, I., "Theoretical Investigation of a Humidification Dehumidification Desalination System Configured by a Double Pass Flat Plate Solar Air Heater", Desalination, Vol.205, pp.163-177, 2007.

[9] Marmouch, H., Orfi, J., and Ben Nasrallah, S., 2007."Effect of a Cooling Tower on a Desalination System", Desalination 238: 281-289.

[10] Dai, Y.J., Wang, R.Z., and Zhang, H.F., "Parametric Analysis to Improve the Performance of a Solar Desalination Unit with Humidification and Dehumidification", Desalination, Vol.142, pp.107-118, 2002.

[11] Gao, P. Zhang, L., and Zhang, H., "Performance Analysis of a New Type Desalination Unit of Heat Pump with Humidification and Dehumidification", Desalination, Vol.202, pp. 531-537, 2008.

[12] Garg, H.P., Adhikari, R.S., and Kumar, R., "Experimental Design and Computer Simulation of Multi-Effect Humidification (MEH)–Dehumidification Solar Distillation", Desalination, Vol.153, pp. 81-86, 2002.

[13] Fath H.S., and Ghazy A., "Solar Desalination Using Humidification–Dehumidification", IWT C, Alexandria, Egypt, 2000.

[14] Darwish M.A.," Experimental and Theoretical Study of Humidification – Dehumidification Desalting System", Desalination, Vol.94, pp.11–24.

[15] Al-Hallaj S., and Farid, M., "Solar Desalination with a Humidification–Dehumidification Cycle: Performance Unit", Desalination, Vol.120, pp. 273–280, 1998.

[16] Moustafa M., Elsayed, Ibrahim S. Taha, and Jaffer A.Sabbagh,"Design of Solar Thermal Systems", Jeddah, Saudi Arabia, 1994.

[17] John A., William, D. and Beckman, A., "Solar Engineering of thermal processes", New York, USA: John Wiley, 1980.

[18] Maclaine-cross, I.L. and P.J. Banks, "A general theory of wet surface heat exchanger and its application to regenerative evaporative cooling". ASME J. Heat Trans., Vol.103, pp.579-585, 1981.

[19] Kettleborough, C.F., and C.S. Hsieh, "The Thermal Performance of the Wet Surface Plastic Plate Heat Exchanger Used as an Indirect Evaporative Cooler", ASME J. Heat Transfer, Vol.105 (2), pp. 366-375, 1983.

[20] Tchinda R, 2009."A review of the mathematical models for predicting solar air heaters systems" Renewable and sustainable energy reviews, Vol.640, pp.1–26, 2009.